

Dalton Transactions

Accepted Manuscript



This is an *Accepted Manuscript*, which has been through the Royal Society of Chemistry peer review process and has been accepted for publication.

Accepted Manuscripts are published online shortly after acceptance, before technical editing, formatting and proof reading. Using this free service, authors can make their results available to the community, in citable form, before we publish the edited article. We will replace this *Accepted Manuscript* with the edited and formatted *Advance Article* as soon as it is available.

You can find more information about *Accepted Manuscripts* in the [Information for Authors](#).

Please note that technical editing may introduce minor changes to the text and/or graphics, which may alter content. The journal's standard [Terms & Conditions](#) and the [Ethical guidelines](#) still apply. In no event shall the Royal Society of Chemistry be held responsible for any errors or omissions in this *Accepted Manuscript* or any consequences arising from the use of any information it contains.



Nucleophilic reactivity and electrocatalytic reduction of halogenated organic compounds by nickel *o*-phenylenedioxamate complexes

Received 00th January 20xx,
Accepted 00th January 20xx

DOI: 10.1039/x0xx00000x

www.rsc.org/

Siva Prasad Das,^a Rakesh Ganguly,^a Yongxin Li,^a and Han Sen Soo^{*,a,b,c}

A growing number of halogenated organic compounds have been identified as hazardous pollutants. Although numerous advanced oxidative processes have been developed to degrade organohalide compounds, reductive and nucleophilic molecular approaches to dehalogenate organic compounds have rarely been reported. In this manuscript, we employ nickel(II) –ate complexes bearing the *o*-phenylenebis(*N*-methyloxamide) (Me₂opba) tetraanionic ligand as nucleophilic reagents that can react with alkyl halides (methyl up to the bulky isobutyl) by *O*-alkylation to give their respective imidate products. Four new nickel(II) complexes have been characterized by X-ray crystallography, and the salient structural parameters and FT-IR vibrational bands (~1655 cm⁻¹) concur with their assignment as the imidate tautomeric form. To the best of our knowledge, this is the first report on the nucleophilic reactivity of Ni^{II}(Me₂opba) with halogenated organic compounds. The parent nickel(II) Me₂opba complex exhibits reversible electrochemical oxidation and reduction behavior. As a proof of concept, Ni^{II}(Me₂opba) and its alkylated congeners were utilized for the electrocatalytic reduction of chloroform, as a representative, simple poly-halogenated organic molecule that could arise from oxidative treatment of organic compounds by chlorination. Modest turnover numbers of up to 6 were recorded, with dichloromethane identified as one of the possible products. Future efforts are directed towards bulkier –ate complexes that possess *metal-centered* instead of ligand-centered nucleophilic activity to create more effective electrocatalysts for the reduction of halogenated organic compounds.

Introduction

There has been constant interest in the utilization of bioinspired redox reagents to facilitate catalytic processes, such as cobalamin for chemical dehalogenation,¹⁻³ Ni-hydrogenases for H₂ evolution,^{4, 5} and P450 mimics and non-heme iron oxo complexes for alkane C-H activation.^{6, 7} Related to this context, a number of research groups have described their efforts in applying bioinspired, more eco-friendly, molecular and electrochemical oxidative approaches to degrade halogenated organic compounds.⁸⁻¹² This is a timely response to a dramatic number of reports that have lately highlighted the detection and persistence of halogenated organic compounds in the environment.¹³⁻²⁶ A few of these

common halogenated organic compounds are listed in Chart S1 (Electronic Supplementary Information, ESI). For example, chloroform is a common by-product from chlorine oxidations,²⁷ which has been linked to the depression of the central nervous system, mental confusion, and even cancer.²⁸ In this context, electrocatalytic hydrogenation or reduction by materials has been found to be somewhat effective.²⁹⁻³² However, there has been a dearth of research on molecular reductive or nucleophilic procedures to remove halogenated organic compounds,³³ with the majority of efforts focused on biotechnological solutions to convert organic compounds to biogas under anoxic conditions.³⁴

Recently, our team has been involved in the development of solutions for environmental applications^{35, 36} and energy research³⁷⁻³⁹ utilizing exclusively Earth-abundant elements. We have employed mesoporous cerium oxide nanomaterials for the photocatalytic oxidative degradation of rhodamine B, via reactive oxygen species such as hydroxyl and hydroperoxy radicals.³⁶ On the other hand, we have exploited a nickel salicylaldimine electrocatalyst in its reduced –ate form for H₂ evolution from seawater.³⁸ With these prior studies, we considered whether suitable nucleophilic, molecular catalysts that involve late first-row transition metals can be designed for the photo- or electrocatalytic reduction of halogenated organic

^a Division of Chemistry and Biological Chemistry, School of Physical and Mathematical Sciences, Nanyang Technological University, 21 Nanyang Link 637371, Singapore. E-mail: hansen@ntu.edu.sg

^b Singapore-Berkeley Research Initiative for Sustainable Energy (SinBeRISE), 1 Create Way, Singapore 138602.

^c Solar Fuels Laboratory, Nanyang Technological University, 50 Nanyang Avenue, Singapore 639798.

† Electronic Supplementary Information (ESI) available: General information on the materials and methods, preparation of the ligand, detailed information on the synthesis and characterization of the remaining new complexes, electrochemical experiments, cyclic voltammograms, crystallographic data and collection parameters, and selected bond lengths and angles (PDF). X-ray crystallographic data for **3a-d** in CIF format (CIF). See DOI: 10.1039/x0xx00000x

ARTICLE

Dalton Transactions

compounds, as a different approach to degrade these oxidized pollutants.

Among nucleophilic, late, first row transition metal complexes, reduced cobalamin derivatives are reputed to be “supernucleophilic” even under aqueous conditions.¹ There have been a small number of reports where cobalamin was used for dehalogenation reactions. Some functionalized TiO₂-cobalamin hybrid materials^{2, 3, 40} as well as heme-based composites^{41, 42} have shown activity for the dechlorination of 1,1-bis(4-chlorophenyl)-2,2,2-trichloroethane (DDT). Other related reductants comprising molecular reactivity include cobalt phthalocyanine-TiO₂ composites for dehalogenation of CHBr₃,⁴³ “hydrated electrons” derived from ruthenium tris(bipyridine),⁴⁴ and metal carbonyls in the dechlorination of CCl₄ and CHCl₃.⁴⁵ A common theme among these rare examples of reductive dehalogenation processes is the presence of molecules as electronic reservoirs, frequently with late transition metal -ate complexes.^{1, 3, 40-46}

In light of these limited number of related studies, we sought a readily synthesized, multidentate, anionic ligand that can support late first-row transition metals as -ate complexes. The family of *o*-phenylenebis(*N*-alkyloxamide) ligands are tetraanionic and can be prepared in two steps from commercially available reagents. The complexes comprising *o*-phenylenebis(*N*-methyloxamide) (Me₂opba) (**1**) have been typically Co, Ni, or Cu compounds that have been applied as oxidative catalysts in alcohol oxidation, decarboxylation, and epoxidation of olefins, possibly due to the accessible higher valent intermediates mediated by the tetraanionic ligand.⁴⁷⁻⁵⁴ Although a number of nucleophilic -ate complexes comprising 3d transition metals exist,⁵⁵⁻⁶³ however, to the best of our knowledge, the nucleophilic *O*-alkylation reactivity of Me₂opba in -ate complexes has not been reported so far. Herein, we present for the first time Ni^{II}(Me₂opba) as a nucleophilic reagent in reactions with halogenated organic compounds. The products isolated from the stoichiometric reactions have been characterized by single crystal X-ray structural analysis, electrochemistry, and FT-IR spectroscopy. As a proof of principle, we have included results for the electrocatalytic reduction of CHCl₃ (as a representative poly-halogenated organic compound) with the Ni^{II} complexes. The modest catalytic performances allude to the need for more sterically encumbering ligand designs to preserve longer-term electrocatalytic activity by avoiding reactivity at the ligand.

Results and discussion

The preparation of [N(Me)₄]₂[Ni^{II}(Me₂opba)] (**2**) is identical to previous procedures, with modifications to the scale, as shown in Schemes S1 and S2 (ESI).^{47, 48, 54} We have fully characterized **2** and found that the spectroscopic properties match those found in a previously reported study.⁵⁴ In addition, we have conducted cyclic voltammetry of **2** in acetonitrile (MeCN, Fig. 1 and S20 (ESI)) and DMSO, using *n*-Bu₄NPF₆ and KPF₆ as the supporting electrolytes, respectively. The cyclic voltammograms are found to be comparable in both solvents. The electrochemical data are

summarized in Table 1. The E_{1/2} values of -0.27 and +0.47 V (vs Fc⁺/Fc) correspond to the Ni^{III}/Ni^{II} and subsequent formation of the ligand cation radical respectively, as reported earlier.⁵⁴ However, an unreported *new additional wave* was observed at E_{1/2} of -2.42 V, which may be attributed to the Ni^{II}/Ni^I redox couple. This Ni^{II}/Ni^I redox couple was found to be reversible (Fig. 1b). The two small peaks at around -1.20 and -1.66 V in the anodic direction (Fig. 1a) likely arise from solvent degradation by-products upon applying reductive potentials down to -3.0 V, beyond the Ni^{II}/Ni^I redox couple. This was verified in a separate CV experiment when the potential was reversed at -2.18 V. Under this condition, both small anodic peaks were absent.

Subsequently, **2** was mixed with excess amounts of alkyl iodides (R-I; R = Me, Et, ⁱPr, ^tBu) in MeCN at 35 to 45 °C (Scheme 1). After at least 72 h, the pale yellow solutions of **2** turned pink. Moreover, the NMR spectra of the reaction mixtures indicated that the ligand in the complexes had desymmetrized, confirming that **2** had been consumed in the reaction with the alkyl iodides. The ¹H and ¹³C NMR spectra suggested that **2** had been alkylated to form diamagnetic products, **3a-d** (**3a** = Me, **3b** = Et, **3c** = ⁱPr, and **3d** = ^tBu). The spectra are presented in Fig. S5 – S12 (ESI). Characteristic peaks for methoxy, ethoxy, isopropoxy, and isobutoxy groups were observed in the ¹H NMR spectra for **3a – 3d**, respectively (Table 2). These results strongly suggest that *O*-alkylation of an amide group in **2** had occurred, instead of alkylation at Ni or elsewhere in the ligand. Likewise, new peaks appeared for the methoxy, ethoxy, isopropoxy, and isobutoxy groups in the ¹³C NMR spectra of **3a-3d**, respectively (Table 2). Besides these, distinct peaks were detected for each carbon of the amides and aromatic groups due to the asymmetry

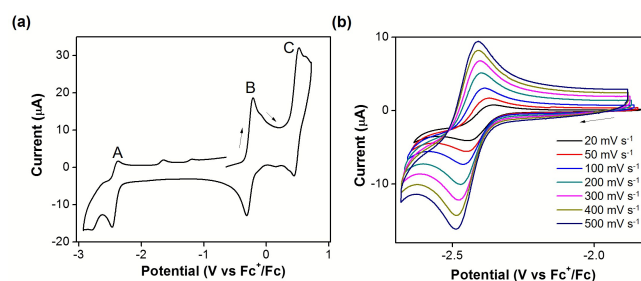
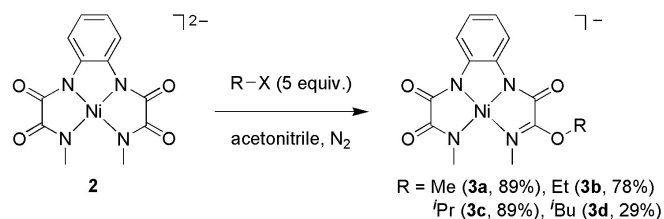


Fig. 1 Cyclic voltammogram of **2** (1.0 mM) in MeCN using *n*-Bu₄NPF₆ (0.10 M) as the electrolyte at (a) scan rate = 100 mV s⁻¹ for the accessible solvent window (A, B and C stand for the Ni^{II}/Ni^I and Ni^{III}/Ni^{II} redox couples, followed by formation of the ligand-based cation radical, respectively); (b) different scan rates for the Ni^{II}/Ni^I redox couple. The arrows indicate the directions of the scans.

Table 1 Electrochemical data for the complexes **2** and **3** (0.10 mM) in MeCN using *n*-Bu₄NPF₆ (0.10 M) as the electrolyte at a scan rate = 100 mV s⁻¹.^a

Complex	E _p ^{ox} / E _p ^{red} (V vs Fc ⁺ /Fc)		
2	-2.38/-2.46	-0.21/-0.32	0.49/0.44
3a	-2.34/-2.44	0.15/0.09	0.78/-
3b	-2.33/-2.46	0.15/0.08	0.77/-
3c	-2.32/-2.44	0.17/0.11	0.77/-
3d	-2.38/-2.47	0.16/0.09	0.83/-

^a E_p^{ox} and E_p^{red} represent the oxidation and reduction peak potentials respectively.



Scheme 1 Nucleophilic reaction of **2** with alkyl halides RX (R = Me, Et, ⁱPr, ^tBu; X = Br, I).

Table 2 Chemical shifts for methoxy, ethoxy, isopropoxy, and isobutoxy group in the complexes **3a-3d**, respectively.

Complex	Chemical shift (ppm)	
	¹ H NMR	¹³ C NMR
3a	4.35 (CH ₃)	60.4 (CH ₃)
3b	1.32 (CH ₃) 4.88 (CH ₂)	16.3 (CH ₃) 69.2 (CH ₂)
3c	1.32 (2 x CH ₃) 6.08 (CH)	23.6 (2 x CH ₃) 76.5 (CH)
3d	0.97 (2 x CH ₃) 1.98 (CH) 4.64 (CH ₂)	19.0 (2 x CH ₃) 30.1 (CH) 78.8 (CH ₂)

in the ligand environment after *O*-alkylation of one amide donor. Patently, **2** is capable of nucleophilic reactivity even with secondary and more sterically hindered alkyl iodides, although elevated temperatures are required.

After the workup of each reaction mixture followed by recrystallization, single crystals of the alkylated derivatives **3** were isolated and examined by X-ray crystallographic experiments. As illustrated in Fig. 2, the alkyl groups are attached to the oxygen of a *N*-methyloxamide moiety in an overall nucleophilic substitution reaction by **2** on the alkyl iodides. From the single-crystal structural studies, the complexes **3a-3d** were observed to be isostructural and had crystallized (from different solvent combinations) in the monoclinic crystal system, although the crystals were not isomorphous. The salient crystallographic experimental data for the complexes **3a-3d** are given in the ESI, and some of the selected bond lengths and angles are listed in Table 3 and the ESI. All the Ni-N bond distances are similar and range from 1.83 Å to 1.93 Å. The two Ni-N bonds corresponding to the phenylenediimine moiety are slightly shorter than the other two remaining Ni-N bonds. Critically, the C-N bond lengths of the alkylated *N*-methyloxamide group are found to be shortest while the C-O bond lengths are the longest, among the C-N and C=O bonds, respectively. These observations are consistent with the imidate ester tautomeric form for the alkylated *N*-methyloxamide groups (Fig. 2e). Similar C-N and C-O bond lengths have been reported in Ni^{II}-imidate complexes,⁶⁴⁻⁶⁶ which reinforce our assignment of the complexes as the imidate ester tautomer after alkylation. Besides this, similar N-C bond lengths for the remaining unreacted parts of the ligand have been reported previously for Ni^{II} Schiff base complexes.⁶⁷⁻⁶⁹

IR spectroscopy verified the alkylation of a *N*-methyloxamide group in **2** to the imidate ester in each of the complexes **3a-3d**. The IR spectra of **2** and **3a-3d** are presented in Fig. 3. New vibrational bands appeared for **3a-3d** around 1650 cm⁻¹, which were absent or hidden in the broad umbrella of the parent complex **2** (Table 4). These bands can be assigned to the ν(C=N) stretch,^{64, 65} in line with the single crystal X-ray structures. In addition, the unreacted ν(C=O) frequencies of **2** were blue-shifted after alkylation (Table 4). Similar blue-shifts were reported for the ligand Me₂opba after replacing Ni^{II} with Cu^{II}, due to reduced π delocalization of the C=O bond of the oxalyl amide fragment.⁵⁴

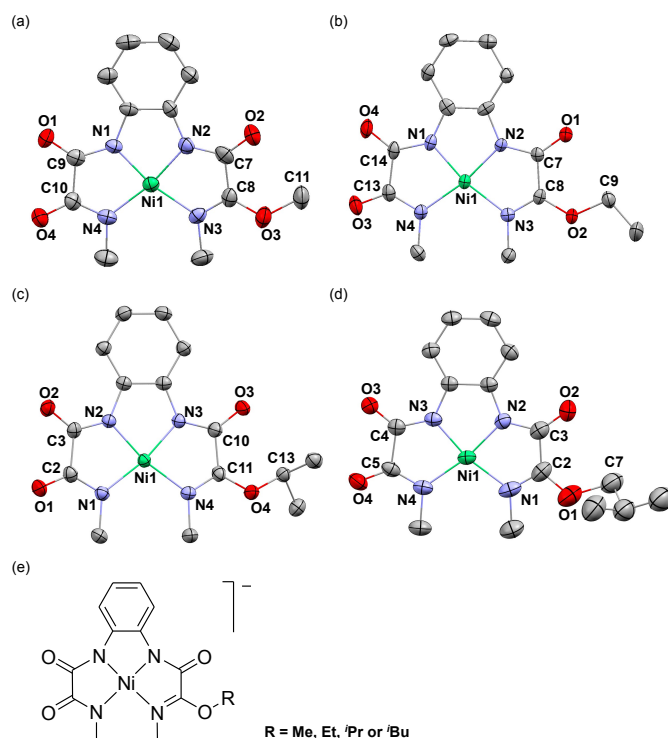


Fig. 2 Single crystal X-ray structures of (a) **3a**, (b) **3b**, (c) **3c**, (d) **3d**, and (e) nominal resonance structures of the alkylated complexes **3**. All the protons and the NMe₄⁺ cation have been omitted for clarity.

Table 3 Selected bond lengths (Å) and angles (°) for complexes **3a-3d**.

Complex	Bond length (Å)	Bond angle (°)
3a	C8-N3 1.288(7)	N3-C8-O3 119.2(6)
	C8-O3 1.330(7)	N3-C8-C7 115.8(6)
		O3-C8-C7 125.0(6)
3b	C8-N3 1.300(5)	N3-C8-O2 118.3(4)
	C8-O2 1.334(5)	N3-C8-C7 117.2(4)
		O2-C8-C7 124.5(4)
3c	C11-N4 1.293(3)	N4-C11-O4 119.9(3)
	C11-O4 1.331(3)	N4-C11-C10 116.4(2)
		O4-C11-C10 123.7(2)
3d	C2-N1 1.299(5)	N1-C2-O1 110.1(8)
	C2-O1 1.315(18)	N1-C2-C3 117.5(3)
		O1-C2-C3 131.7(9)

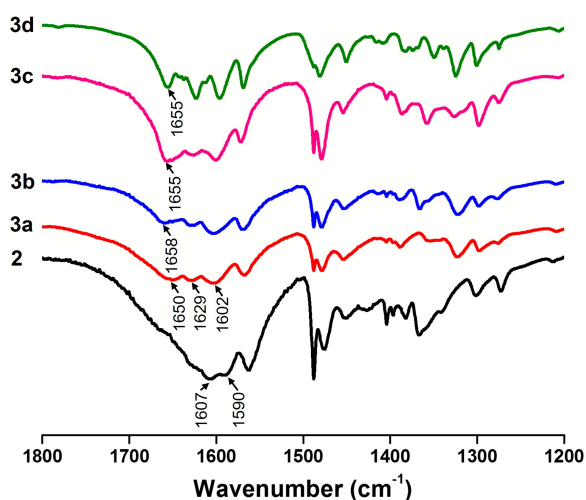


Fig. 3 FT-IR spectra of **2** (black), **3a** (red), **3b** (blue), **3c** (pink), and **3d** (green) in the range of 1200 – 1800 cm^{-1} .

Table 4 Infrared spectral data for complexes **2** and **3a-3d**.

2	Complex				Assignment
	3a	3b	3c	3d	
1590	1602	1603	1601	1595	ν(C=O)
1607	1629	1629	1626	1623	
	1650	1658	1655	1655	ν(C=N)

The UV-visible spectra for **2** and **3a-3d** were recorded in MeCN and presented in Fig. S31, and the λ_{max} values are summarized in Table S1. The absorption peaks for **2** matched those reported previously.⁵⁴ The higher energy electronic transition in the UV region at 255 nm can be ascribed to intraligand (IL) $\pi-\pi^*$ transitions of the phenylenediimine motif, whereas the absorption at 357 nm is due to metal-to-ligand charge transfer (MLCT) transitions.⁵⁴ Besides these, the broad shoulder in the range 410-465 nm is attributed to superpositions of $d-d$ transitions from the filled d orbitals to the empty LUMO of the Ni^{II} complex in the square-planar geometry.⁵⁴ However, there is a blue-shift for these peaks after alkylation of **2**. The IL, MLCT, and $d-d$ bands appeared in the range of 250-252, 308-310, and 359-362 nm, respectively for **3a-3d**. This could arise from the weaker π -donor, and conversely, more effective π -acceptor properties of the imidate ester tautomeric form, which increases the gap between the d orbitals among complexes **3a-3d**.

The by-product in the reaction of **2** with one of the alkyl iodides was conclusively identified by NMR spectroscopy and electrospray ionization-mass spectrometry (ESI-MS). In a representative reaction, after isolation of the product **3a** from the reaction between **2** and methyl iodide, the solid residue remaining in the reaction flask was washed with hexane and dried *in vacuo*. The ^1H NMR spectrum and ESI-MS of the dried residue are shown in Fig. S32 - S34 (ESI). The ^1H NMR spectrum showed a singlet at $\delta = 3.09$, which corresponds to Me_4N^+ cation. Apart from this, there were no additional peaks in the range of $\delta = -1$ to 22. This confirmed the presence of Me_4N^+

as the sole organic part in the solid. The ESI-MS displayed prominent signals at $m/z = 126.83$ and 74.22 Da in the negative (Fig. S33) and positive (Fig. S34) ion modes, respectively. These m/z values corresponded to I^- for the former and Me_4N^+ for the latter signals, and strongly indicate that the major by-product was Me_4NI .

We have also explored the reactivity of **2** with organic bromides such as bromoethane and 2-bromopropane. The detailed procedures and the related spectral characterizations for these reactions are given in the ESI. It is evident from Fig. S13 and S14 that each of the substrate reacted with **2** and formed their corresponding alkylated products. The chemical shift values for the new products were found to be identical with that of **3b** and **3c**, respectively, regardless of the use of the iodo or bromo alkane. Beside ^1H NMR spectroscopy, the ESI-MS recorded for the reaction mixture showed peaks at $m/z = 361.04$ and 374.85 , which also matched the values for the monoanionic $[\mathbf{3b}]^-$ and $[\mathbf{3c}]^-$, respectively. Notably however, the reactions of **3** with the bromoalkanes were slower and gave lower conversions, likely because Br^- is a poorer leaving group than I^- .

Beside these, we have further explored the reaction of **2** with 2-bromoethanol, benzyl bromide, and bromotrichloromethane (BrCCl_3). From Fig. S15, we observed that **2** reacted with 2-bromoethanol to form at least one new product **3e**, which seemed consistent with a similar nucleophilic substitution of the bromide by the amide of **2**. However, **3e** appeared to be hydrolytically unstable even at 0°C , and only the demetallated ligand, **1**, remained after one week. Similarly, the reaction of **2** with benzyl bromide also led to an intractable product mixture (Fig. S17). Consequently, we could not isolate the pure product in either case. Interestingly, upon mixing **2** with BrCCl_3 , there was a distinct color change of the reaction mixture from yellow to brown. However, the product appeared to be paramagnetic, since the signals for **2** vanished within 10 minutes with no new peaks from -100 to $+100$ ppm (Fig. S16). Unfortunately, multiple attempts to isolate single crystals that are suitable for X-ray diffraction have not been successful so far, although we propose that **2** has probably been oxidized to form a brominated Ni(III) product (**3f**). Our attempts to trap the $\bullet\text{CCl}_3$ radical with the help of EPR spectroscopy at room temperature have also been unsuccessful due to its high reactivity. Besides these, we were unable to observe C_2Cl_6 in the reaction mixture by GC-MS. We have also attempted the reaction of pentafluoropyridine with **2** in MeCN. The ^1H and $^{19}\text{F}\{\text{H}\}$ NMR spectra recorded at different time intervals are shown in Fig. S18 and S19, respectively. The new peaks in the spectra indicated that **2** had reacted with pentafluoropyridine, although the mass spectrum mainly showed the presence of mainly **2**. Consequently, we cannot conclusively identify the product.

Cyclic voltammetry experiments of **3a-3d** were performed to examine the redox properties of **2** after alkylation. The CVs were conducted in DMSO and MeCN using KPF_6 and $n\text{-Bu}_4\text{NPF}_6$, respectively, as the supporting electrolyte under an atmosphere of argon (Ar). The CVs for the complexes are shown in Fig. 4 and Fig. S21-S24 (ESI) and the electrochemical data are summarized in Table 1. The cyclic voltammogram of **3a** consists of a reversible wave at $E_{1/2}$ of 0.12 V (Fig. 4a) and a quasi-reversible wave at E_p^{ox} value of 0.78 V (Fig. S21), which corresponds to the $\text{Ni}^{\text{III}}/\text{Ni}^{\text{II}}$ and ligand-based

cation radical redox couples, respectively. These values are shifted anodically by about 390 and 310 mV compared to their corresponding potentials in **2**. This different redox behavior likely arises since **3a** is monoanionic, whereas **2** is a more electron-rich dianionic –ate complex. Beside these, the cyclic voltammogram of **3a** consists of a quasi-reversible wave at $E_{1/2}$ of -2.39 V due to the $\text{Ni}^{\text{III}}/\text{Ni}^{\text{II}}$ redox couple. The position of this redox couple surprisingly appeared to be similar to that of **2**. The peak-to-peak separation for the $\text{Ni}^{\text{III}}/\text{Ni}^{\text{II}}$ and $\text{Ni}^{\text{III}}/\text{Ni}^{\text{I}}$ couples in **3a** have been found to be 60 mV and 100 mV, respectively, compared to almost identical peak-to-peak separations of 90 mV in the corresponding redox couples of **2**.

Similar to **3a**, the complexes **3b-3d** showed $\text{Ni}^{\text{III}}/\text{Ni}^{\text{I}}$, $\text{Ni}^{\text{III}}/\text{Ni}^{\text{II}}$, and ligand-based cation radical redox couples at around -2.40 , 0.13 and 0.79 V, respectively, in their cyclic voltammograms. The $\text{Ni}^{\text{III}}/\text{Ni}^{\text{II}}$ redox couples are found to be reversible whereas the $\text{Ni}^{\text{III}}/\text{Ni}^{\text{I}}$ and ligand-based cation radical redox couples are quasi-reversible (Fig.

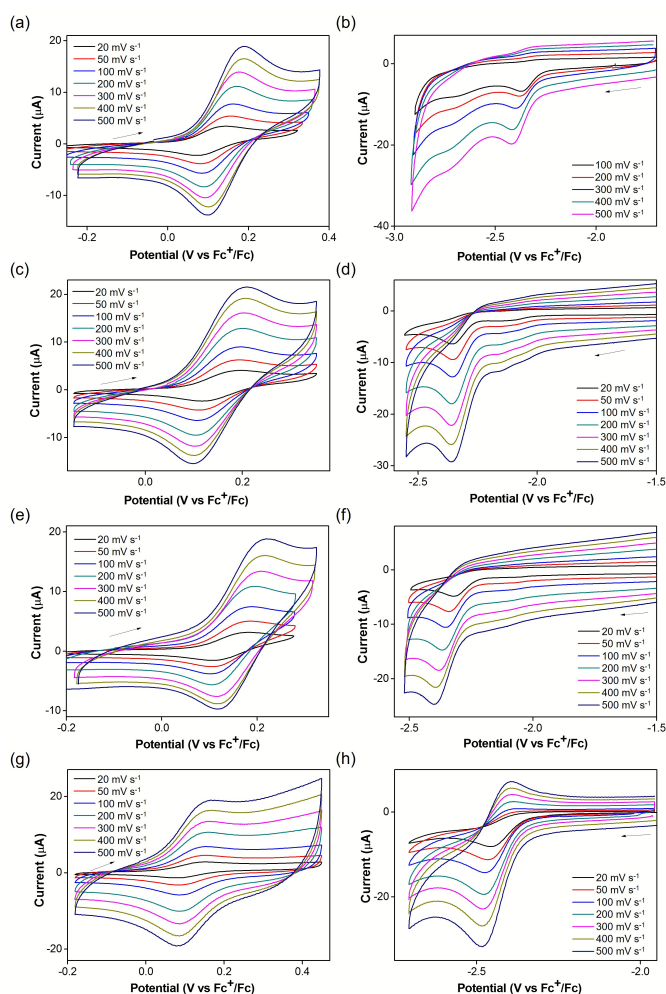


Fig. 4 Cyclic voltammograms for **3a-3d** at different scan rates. (a) $\text{Ni}^{\text{III}}/\text{Ni}^{\text{II}}$ redox couple and (b) $\text{Ni}^{\text{III}}/\text{Ni}^{\text{I}}$ redox couple for **3a** (with 0.10 M KPF_6 in DMSO); (c) $\text{Ni}^{\text{III}}/\text{Ni}^{\text{II}}$ redox couple and (d) $\text{Ni}^{\text{III}}/\text{Ni}^{\text{I}}$ redox couple for **3b** (with 0.10 M KPF_6 in DMSO); (e) $\text{Ni}^{\text{III}}/\text{Ni}^{\text{II}}$ redox couple and (f) $\text{Ni}^{\text{III}}/\text{Ni}^{\text{I}}$ redox couple for **3c** (with 0.10 M KPF_6 in DMSO); (g) $\text{Ni}^{\text{III}}/\text{Ni}^{\text{II}}$ redox couple and (h) $\text{Ni}^{\text{III}}/\text{Ni}^{\text{I}}$ redox couple for **3d** (with 0.10 M $n\text{-Bu}_4\text{NPF}_6$ in MeCN). The arrows indicate the directions of the scans.

4). The relative oxidative stabilities of **2** and **3a-3d**, as suggested by their reversible $\text{Ni}^{\text{III}}/\text{Ni}^{\text{II}}$ oxidation waves, attest to the robustness of Me_2opba as a ligand, and corroborate the previous reports on their applications in oxidation catalysis, including even water oxidation.⁴⁷⁻⁵⁴

With these complexes in hand, we explored the electrocatalytic reduction of CHCl_3 in the absence and presence of protic solvents. In preliminary experiments, CVs were carried out with CHCl_3 and isopropyl alcohol (IPA) in the presence or absence of the catalyst in DMSO using KPF_6 (0.10 M) as the supporting electrolyte (Fig. S25-S28). From the CVs it was found that the solvent reduction current increased only slightly in the presence of **2** (Fig. S25). Interestingly, with the alkylated complexes **3**, the onset potential was shifted positively (Fig. S26-S28), probably due to the monoanionic charges of **3** as opposed to the dianionic **2**. With these encouraging observations, we conducted controlled potential electrolysis (CPE) experiments for the reduction of CHCl_3 . The results are summarized in Table 5. The conversions were calculated on the basis of ^1H NMR spectra recorded for aliquots taken out from the reaction mixture before and after electrolysis. Benzene was used as an internal standard for each CPE experiment.

At the beginning, electrocatalytic reduction of CHCl_3 was conducted in the absence of protic solvents by using **2** as the catalyst at -2.5 V for 30 min (vs Fc^+/Fc , Table 5, entry 2). Only 3% conversion was detected. In a separate experiment, the reaction was repeated in the presence of IPA (2 equivalents relative to the CHCl_3 substrate) as the proton source and the conversion was found to increase by three-fold (Table 5, entry 3). We also explored the reactivity of the complexes in the presence of water or methanol as the proton sources, but the conversion did not increase (Table 5, entries 4 and 5). Notably, in the control experiment conducted under similar reaction conditions using IPA as the proton source but in the absence of **3**, only 2% conversion of CHCl_3 was observed (Table 5, entry 1). This indicated that the complex played an important role in the electrolysis.

We have further carried out the CPE measurements using **3a-3d** as the catalysts in the presence of IPA and found that the conversions range from 9 to 11%, corresponding to TONs of 4.7 to 5.6 (Table 5, entries 6-9). Under otherwise identical CPE conditions, increasing the reaction time with or without **2** or **3** as the catalyst up to 2 h did not increase the conversion. We also identified trace amounts of dichloromethane as the product in the ^1H NMR spectra (Fig. S30). Though the complexes **2** and **3** showed only modest conversions in comparison to previous reports on the electrocatalytic reduction of organic halides by metal complexes,^{32, 70-75} further work to improve the conversion and also identify other products, such as H_2 , are under way in our team.

Table 5 Electrocatalytic reduction of CHCl_3 by the complexes **2** and **3**.^a

Entry	Complex	Conversion (%)	TON
1 ^b	none	2	
2 ^c	2	3	1.6
3	2	10	5.0
4 ^d	2	6	3.2
5 ^e	2	6	3.0
6	3a	9	4.7
7	3b	11	5.6
8	3c	9	4.7
9	3d	11	5.6

^a All CPE experiments were conducted in DMSO (15 mL) using KPF_6 (0.10 M) as the supporting electrolyte at -2.5 V for 30 min (50 mM benzene, 50 mM CHCl_3 , 100 mM *iso*-propyl alcohol, and 1.0 mM complex under argon), unless otherwise indicated. ^b No catalyst added. ^c No protic solvent. ^d Water as proton source. ^e Methanol as proton source.

Experimental

General information

All the new Ni(II) complexes, **3a-d** were synthesized by using standard Schlenk line techniques under N_2 , unless otherwise indicated. The chemicals, including anhydrous dimethyl sulfoxide (DMSO), were purchased from Sigma-Aldrich, Alfa-Aesar, and Tokyo Chemical Industry (TCI), and were used as received. The deuterated solvents were purchased from Cambridge Isotope Laboratories and were used as received. Anhydrous acetonitrile (MeCN) was obtained from a PURE SOLV MD-5 solvent purification system (Innovative Technology, Inc.).

The NMR spectra were acquired at room temperature on either a Bruker AVANCE 300 MHz or 500 MHz spectrometer. The chemical shift (δ) values are reported in parts per million (ppm) relative to residual solvent peaks ($\text{CDCl}_3 = 7.26$ ppm for ^1H and 77.2 ppm for ^{13}C ; $\text{CD}_3\text{CN} = 1.94$ ppm for ^1H and 118.3 ppm for ^{13}C ; $\text{MeOD-}d_4 = 3.31$ ppm for ^1H and 49.2 ppm for ^{13}C ; $\text{DMSO-}d_6 = 2.50$ ppm for ^1H and 39.52 ppm for ^{13}C). Crystallographic data were recorded on a Bruker X8 CCD diffractometer. The structures were solved and refined using the Bruker SHELXTL software package. High-resolution electrospray ionization mass spectra (HR-ESIMS) were obtained using a Waters Q-ToF Premier mass spectrometer. Infrared spectra of the samples were recorded as KBr pellets using a Bruker VERTEX 80 spectrophotometer.

Preparation of compound $(\text{Me}_4\text{N})_2[\text{Ni}(\text{Me}_2\text{opba})]$ (**2**)

Complex $(\text{Me}_4\text{N})_2[\text{Ni}(\text{Me}_2\text{opba})]$ (**2**) was prepared by using the procedure previously reported.⁵⁴ In a typical experiment, a 25% aqueous solution of $(\text{Me}_4\text{N})\text{OH}$ (1.31 mL, 3.60 mmol) was added to a suspension of **1** (0.200 g, 0.72 mmol) in methanol (15 mL). The mixture was heated at 50 °C and stirred till it became clear. The solution was cooled to room temperature and a $\text{Ni}(\text{ClO}_4)_2 \cdot 6\text{H}_2\text{O}$ (0.26 g, 0.72 mmol) solution in methanol (10 mL) was added dropwise under stirring. The reaction mixture was filtered to remove the precipitated $(\text{Me}_4\text{N})\text{ClO}_4$. Subsequently, the volume of the red solution was reduced to one-third under reduced pressure. Diethyl ether and acetone were successively added to the final deep

red solution to precipitate a yellow to orange solid. The solid was filtered off and dried *in vacuo* to yield pure **2** (0.383 g, 79.9%). The product identity has been confirmed by NMR spectroscopy and HR-ESI-MS. ^1H NMR ($\text{MeOH-}d_4$, 300 MHz): $\delta = 2.60$ (s, 6 H), 3.17 (s, 24 H), 6.68 (dd, $J = 3.3, 6.0$ Hz, 2 H), 8.03 (dd, $J = 3.3, 6.0$ Hz, 2 H). $^{13}\text{C}\{^1\text{H}\}$ NMR ($\text{MeOD-}d_4$, 126 MHz): $\delta = 34.2, 56.1$ (t), 120.7, 123.4, 144.7, 166.0, 172.1. HRMS (ESI-, m/z) calculated for $\text{C}_{12}\text{H}_{11}\text{N}_4\text{NiO}_4$ $[\text{M} + \text{H}]^-$ $m/z = 333.0134$, found 333.0137.

Reaction of **2** with iodomethane to form **3a** (remaining examples in ESI):

A 2 M solution of iodomethane (226.0 μL , 0.45 mmol) in *tert*-butyl methyl ether was added to a solution of **2** (0.050 g, 0.090 mmol) in 50 mL MeCN under N_2 in a Schlenk tube. The tube was sealed, heated to 35 °C, and stirred for 72 h during which the color changed from yellow to red. After the reaction, the MeCN was removed under reduce pressure, dried *in vacuo*, and washed with hexane (5 mL x 3). The red complex was extracted with acetone (5 mL) twice and the combined acetone extracts were dried under reduced pressure. The crude solid red product was re-dissolved in MeCN (5 mL) and diethyl ether (~5 mL) was added dropwise until some yellow color precipitate appeared. The precipitate was allowed to deposit, before being filtered off. The red filtrate was dried *in vacuo* to provide pure **3a** in high yields (0.032 g, 88.9%). Diffusion of anhydrous diethyl ether into a MeCN solution of the complex gave red crystals that were suitable for single crystal X-ray structural analysis. ^1H NMR (CD_3CN , 300 MHz): $\delta = 2.50$ (s, 3 H), 2.78 (s, 3 H), 3.09 (s, 12 H), 4.35 (s, 3 H), 6.59-6.72 (m, 2 H), 7.97 (dd, $J = 1.5, 7.8$ Hz, 1 H), 8.07 (dd, $J = 1.5, 7.8$ Hz, 1 H). $^{13}\text{C}\{^1\text{H}\}$ NMR (CD_3CN , 126 MHz): $\delta = 32.8, 36.0, 56.2$ (t), 60.4, 119.6, 119.9, 121.6, 123.6, 142.8, 146.0, 160.1, 163.4, 165.8, 171.3. HRMS (ESI-, m/z) calculated for $\text{C}_{13}\text{H}_{13}\text{N}_4\text{NiO}_4$ $[\text{M}]^-$ $m/z = 347.0290$, found 347.0292. Elemental analyses for $\text{C}_{17}\text{H}_{25}\text{N}_5\text{NiO}_4$ calculated: C, 48.37; H, 5.97; N, 16.59%; found: C, 48.35; H, 6.04; N, 16.23%.

Electrochemistry: Cyclic voltammetry

The cyclic voltammetry experiments were carried out by using a Biologic SP-300 potentiostat in anhydrous DMSO or MeCN with 0.10 M KPF_6 or *n*- Bu_4NPF_6 as the supporting electrolyte. A standard three-electrode electrochemical cell was used, consisting of a glassy carbon working electrode (3 mm in diameter from BAS), a Pt wire as the counter electrode, and an Ag/AgCl electrode as a reference electrode or another Pt wire as a pseudo-reference electrode. Ferrocene was used as an internal reference when a Pt wire was used as the pseudo-reference electrode and all the potentials have been reported vs the ferrocenium/ferrocene (Fc^+/Fc) redox couple. The glassy carbon electrode was polished between each run on a polishing pad using a suspension of 0.05 μm alumina and distilled water. This was followed by sonication in distilled water for 10 min, before the electrode was air-dried. Before each electrolysis, the solutions were bubbled with argon for 15 min.

Controlled potential electrolysis (CPE)

The CPE experiments were performed in a sealed glass cell using a glassy carbon rod (10 mm diameter x 15 mm length) as the working electrode, a Pt wire as the counter electrode, and an Ag/AgCl electrode as the reference electrode or another Pt wire as a pseudo-reference electrode. Before each experiment, the glassy

carbon rod was polished and washed as described above. A typical electrolysis was carried out under argon in DMSO (15 mL) with KPF₆ (0.10 M) as the supporting electrolyte, benzene (50 mM) as an internal standard for ¹H NMR spectroscopy, CHCl₃ (50 mM) as the substrate, and the metal complex (1.0 mM) as the catalyst. Before each CPE experiment, argon was bubbled through the reaction mixture for 15 min, which was followed by linear sweep voltammetry (LSV) experiments to confirm that the complexes were pure. Before and after electrolysis, aliquots were removed from the cell with a gas-tight syringe for ¹H NMR spectroscopic measurements.

Conclusions

We have shown that the –ate complex **2**, bearing the tetraanionic ligand **1**, is capable of nucleophilic substitution reactions with alkyl iodides and bromides under slightly elevated temperatures. The products **3** are alkylated at the *N*-methyloxamide oxygen and have been structurally characterized by X-ray crystallography. Furthermore, **2** and **3** function as electrocatalysts in the reduction of CHCl₃, albeit with low TONs. Our results demonstrate the feasibility of a catalytic reductive approach to chemically transform halogenated organic pollutants by using readily prepared –ate complexes composed of Earth-abundant elements. Nevertheless, the catalytic activity of the Ni electrocatalysts are likely to be hampered by irreversible alkylation of the ligand instead of reversible electron transfers from the metal center to the substrate. Ongoing studies in our team include the development of novel Ni –ate molecular systems that are supported by more sterically bulky ligands, which exploit the Ni nucleus instead, as the site for nucleophilic activity.

Acknowledgements

H.S.S. is supported by a NTU start-up grant (M4081012), the Nanyang Assistant Professorship (M4081154), and an MOE Tier 1 grant (M4011144). The authors acknowledge the support from the Solar Fuels Laboratory at NTU and the Singapore-Berkeley Research Initiative for Sustainable Energy (SinBeRISE) CREATE Programme. This research program is funded by the National Research Foundation (NRF), Prime Minister's Office, Singapore under its Campus for Research Excellence and Technological Enterprise (CREATE).

Notes and references

- H. Shimakoshi and Y. Hisaeda, *Angew. Chem. Int. Ed.*, 2015, **54**, 15439-15443.
- H. Shimakoshi, E. Sakumori, K. Kaneko and Y. Hisaeda, *Chem. Lett.*, 2009, **38**, 468-469.
- W. Zhang, H. Shimakoshi, N. Houfuku, X. M. Song and Y. Hisaeda, *Dalton Trans.*, 2014, **43**, 13972-13978.
- C. Y. Lee, H. S. Park, J. C. Fontecilla-Camps and E. Reisner, *Angew. Chem. Int. Ed.*, 2016, **55**, 5971-5974.
- W. Lubitz, H. Ogata, O. Rudiger and E. Reijerse, *Chem. Rev.*, 2014, **114**, 4081-4148.
- W. N. Oloo and L. Que, *Acc. Chem. Res.*, 2015, **48**, 2612-2621.
- M. C. Feiters, A. E. Rowan and R. J. M. Nolte, *Chem. Soc. Rev.*, 2000, **29**, 375-384.
- S. Sen Gupta, M. Stadler, C. A. Noser, A. Ghosh, B. Steinhoff, D. Lenoir, C. P. Horwitz, K. W. Schramm and T. J. Collins, *Science*, 2002, **296**, 326-328.
- C. A. Martinez-Huitle and S. Ferro, *Chem. Soc. Rev.*, 2006, **35**, 1324-1340.
- S. K. Khetan and T. J. Collins, *Chem. Rev.*, 2007, **107**, 2319-2364.
- T. J. Collins, *Acc. Chem. Res.*, 2002, **35**, 782-790.
- S. Kundu, A. Chanda, S. K. Khetan, A. D. Ryabov and T. J. Collins, *Environ. Sci. Technol.*, 2013, **47**, 5319-5326.
- J. M. Carter, M. J. Moran, J. S. Zogorski and C. V. Price, *Environ. Sci. Technol.*, 2012, **46**, 8189-8197.
- B. Rao, N. Estrada, S. McGee, J. Mangold, B. H. Gu and W. A. Jackson, *Environ. Sci. Technol.*, 2012, **46**, 11635-11643.
- Z. L. Fan, J. Y. Hu, W. An and M. Yang, *Environ. Sci. Technol.*, 2013, **47**, 10841-10850.
- Y. Pan and X. R. Zhang, *Environ. Sci. Technol.*, 2013, **47**, 1265-1273.
- D. M. Cwiertny, S. A. Snyder, D. Schlenk and E. P. Kolodziej, *Environ. Sci. Technol.*, 2014, **48**, 11737-11745.
- L. Deng, C. H. Huang and Y. L. Wang, *Environ. Sci. Technol.*, 2014, **48**, 2697-2705.
- K. D. Lin, C. Yan and J. Gan, *Environ. Sci. Technol.*, 2014, **48**, 263-271.
- S. Y. Pang, J. Jiang, Y. Gao, Y. Zhou, X. L. Huangfu, Y. Z. Liu and J. Ma, *Environ. Sci. Technol.*, 2014, **48**, 615-623.
- M. T. Yang and X. R. Zhang, *Environ. Sci. Technol.*, 2014, **48**, 11846-11852.
- H. Y. Zhai, X. R. Zhang, X. H. Zhu, J. Q. Liu and M. Ji, *Environ. Sci. Technol.*, 2014, **48**, 2579-2588.
- M. Venier, A. Salamova and R. A. Hites, *Acc. Chem. Res.*, 2015, **48**, 1853-1861.
- X. W. Wang, X. F. Hu, H. Zhang, F. Chang and Y. M. Luo, *Environ. Sci. Technol.*, 2015, **49**, 6683-6690.
- H. X. Zhao, J. Q. Jiang, Y. L. Wang, H. J. Lehmler, G. R. Buettner, X. Quan and J. W. Ghen, *Environ. Sci. Technol.*, 2015, **49**, 14120-14128.
- Q. Zhao, H. M. Zhao, X. Quan, X. He and S. Chen, *Environ. Sci. Technol.*, 2015, **49**, 9092-9099.
- U. Ali, J. H. Syed, R. N. Malik, A. Katsoyiannis, J. Li, G. Zhang and K. C. Jones, *Sci. Total Environ.*, 2014, **476-477**, 705-717.
- G. Wang, C. Feng, C. Kang, B. Zhang, N. Chen and X. Zhang, *J. Environ. Eng.*, 2016, **142**, 04015066.
- G. Chen, Z. Wang and D. Xia, *Electrochem. Commun.*, 2004, **6**, 268-272.
- H. Cheng, K. Scott and P. A. Christensen, *J. Electroanal. Chem.*, 2004, **566**, 131-138.
- C. Cui, X. Quan, H. Yu and Y. Han, *Applied Catal. B Environ.*, 2008, **80**, 122-128.
- Z. Sun, H. Ge, X. Hu and Y. Peng, *Chem. Eng. Technol.*, 2009, **32**, 134-139.
- D. Sadowsky, K. McNeill and C. J. Cramer, *Environ. Sci. Technol.*, 2014, **48**, 10904-10911.
- C. Ding and J. Z. He, *Microb. Biotechnol.*, 2012, **5**, 347-367.
- S. Gazi, W. K. H. Ng, R. Ganguly, A. M. P. Moeljadi, H. Hirao and H. S. Soo, *Chem. Sci.*, 2015, **6**, 7130-7142.
- S. K. Muduli, S. Wang, S. Chen, C. F. Ng, C. H. A. Huan, T. C. Sum and H. S. Soo, *Beilstein J. Nanotechnol.*, 2014, **5**, 517-523.
- J. W. Kee, Y. Y. Ng, S. A. Kulkarni, S. K. Muduli, K. Xu, R. Ganguly, Y. Lu, H. Hirao and H. S. Soo, *Inorg. Chem. Front.*, 2016, **3**, 651-662.
- H. Shao, S. K. Muduli, P. D. Tran and H. S. Soo, *Chem. Commun.*, 2016, **52**, 2948-2951.
- J. Wang, R. Ganguly, Y. Li, J. Diaz, H. S. Soo and F. Garcia, *Dalton Trans.*, 2016, **45**, 7941-7946.
- H. Shimakoshi and Y. Hisaeda, *ChemPlusChem*, 2014, **79**, 1250-1253.
- S. O. Obare, T. Ito and G. J. Meyer, *J. Am. Chem. Soc.*, 2006, **128**, 712-713.
- J. R. Stromberg, J. D. Wnuk, R. A. F. Pinlac and G. J. Meyer, *Nano Lett.*, 2006, **6**, 1284-1286.
- R. J. Kuhler, G. A. Santo, T. R. Caudill, E. A. Betterton and R. G. Arnold, *Environ. Sci. Technol.*, 1993, **27**, 2104-2111.
- M. Goez, C. Kerzig and R. Naumann, *Angew. Chem. Int. Ed.*, 2014, **53**, 9914-9916.
- E. T. Chukovskaya, M. A. Rozhkova, N. A. Kuzmina and R. K. Freidlina, *Bull. Acad. Sci. USSR Chem. Sci.*, 1982, **31**, 321-325.
- D. A. White, *Synth. React. Inorg. Met.-Org. Chem.*, 1977, **7**, 433-443.
- R. Ruiz, C. Surville-Barland, A. Aukauloo, E. Anxolabehere-Mallart, Y. Journaux, J. Cano and M. C. Munoz, *J. Chem. Soc. Dalton Trans.*, 1997, 745-751.
- I. Fernandez, J. R. Pedro, A. L. Rosello, R. Ruiz, X. Ottenwaelder and Y. Journaux, *Tetrahedron Lett.*, 1998, **39**, 2869-2872.
- G. Blay, I. Fernandez, P. Formentin, B. Monje, J. R. Pedro and R. Ruiz, *Tetrahedron*, 2001, **57**, 1075-1081.
- I. Fernandez, J. R. Pedro, A. L. Rosello, R. Ruiz, I. Castro, X. Ottenwaelder and Y. Journaux, *Eur. J. Org. Chem.*, 2001, 1235-1247.
- R. Carrasco, J. Cano, X. Ottenwaelder, A. Aukauloo, Y. Journaux and R. Ruiz-Garcia, *Dalton Trans.*, 2005, 2527-2538.
- M. A. Abdulmalic, A. Aliabadi, A. Petr, Y. Krupskaya, V. Kataev, B. Buchner, R. Zaripov, E. Vavilova, V. Voronkova, K. Salikov, T. Hahn, J. Kortus, F. E. Meva, D. Schaarschmidt and T. Ruffer, *Dalton Trans.*, 2015, **44**, 8062-8079.
- P. Garrido-Barros, I. Funes-Ardoiz, S. Drouet, J. Benet-Buchholz, F. Maseras and A. Llobet, *J. Am. Chem. Soc.*, 2015, **137**, 6758-6761.
- X. Ottenwaelder, A. Aukauloo, Y. Journaux, R. Carrasco, J. Cano, B. Cervera, I. Castro, S. Curreli, M. C. Munoz, A. L. Rosello, B. Soto and R. Ruiz-Garcia, *Dalton Trans.*, 2005, 2516-2526.
- D.-L. Popescu, A. Chanda, M. Stadler, F. T. de Oliveira, A. D. Ryabov, E. Münck, E. L. Boinaar and T. J. Collins, *Coord. Chem. Rev.*, 2008, **252**, 2050-2071.

ARTICLE

Dalton Transactions

56. M. A. DeNardo, M. R. Mills, A. D. Ryabov and T. J. Collins, *J. Am. Chem. Soc.*, 2016, **138**, 2933-2936.
57. T. J. Collins, R. D. Powell, C. Slebodnick and E. S. Uffelman, *J. Am. Chem. Soc.*, 1991, **113**, 8419-8425.
58. R. W. Hay, R. Bembi and W. Sommerville, *Inorg. Chim. Acta*, 1982, **59**, 147-153.
59. M. Shakir, S. P. Varkey and P. S. Hameed, *Polyhedron*, 1993, **12**, 2775-2780.
60. T. Corona, F. F. Pfaff, F. Acuña-Parés, A. Draksharapu, C. J. Whiteoak, V. Martin-Diaconescu, J. Lloret-Fillol, W. R. Browne, K. Ray and A. Company, *Chem. Eur. J.*, 2015, **21**, 15029-15038.
61. S. Zhu, F. Kou, H. Lin, C. Lin, M. Lin and Y. Chen, *Inorg. Chem.*, 1996, **35**, 5851-5859.
62. M. K. Coggins, M.-T. Zhang, A. K. Vannucci, C. J. Dares and T. J. Meyer, *J. Am. Chem. Soc.*, 2014, **136**, 5531-5534.
63. C. Li, R. K. Thomson, B. Gillon, B. O. Patrick and L. L. Schafer, *Chem. Commun.*, 2003, 2462-2463.
64. S.-G. Kang, J. Song and J. H. Jeong, *Bull. Korean Chem. Soc.*, 2002, **23**, 824-829.
65. S. Bang, N. Kim, S.-G. Kang and J. H. Jeong, *Inorg. Chim. Acta*, 2012, **392**, 184-191.
66. H. Liu, F. Wang, C. Han, H. Zhang, C. Bai, Y. Hu and X. Zhang, *Inorg. Chim. Acta*, 2015, **434**, 135-142.
67. L. Carbonaro, M. Isola, P. La Pegna, L. Senatore and F. Marchetti, *Inorg. Chem.*, 1999, **38**, 5519-5525.
68. J. Costes, J. Lamère, C. Lepetit, P. Lacroix, F. Dahan and K. Nakatani, *Inorg. Chem.*, 2005, **44**, 1973-1982.
69. K. Iwase, Y. Nagano, I. Yoshikawa, H. Houjou, Y. Yamamura and K. Saito, *J. Phys. Chem. C*, 2014, **118**, 27664-27671.
70. A. A. Isse, B. Huang, C. Durante and A. Gennaro, *Applied Catal. B Environ.*, 2012, **126**, 347-354.
71. D. M. Goken, D. G. Peters, J. A. Karty and J. P. Reilly, *J. Electroanal. Chem.*, 2004, **564**, 123-132.
72. K. S. Alleman and D. G. Peters, *J. Electroanal. Chem.*, 1998, **451**, 121-128.
73. A. L. Guyon, L. J. Klein, D. M. Goken and D. G. Peters, *J. Electroanal. Chem.*, 2002, **526**, 134-138.
74. J. D. Persinger, J. L. Hayes, L. J. Klein, D. G. Peters, J. A. Karty and J. P. Reilly, *J. Electroanal. Chem.*, 2004, **568**, 157-165.
75. C. Gosden and D. Pletcher, *J. Organomet. Chem.*, 1980, **186**, 401-409.

Table of contents graphic

Nickel(II) –ate complexes supported by *o*-phenylenebis(*N*-methyloxamide) reacted nucleophilically with alkyl halides to form new imidate tautomers that have been characterized by X-ray crystallography and FT-IR spectroscopy, and utilized for electroreduction of chloroform.

